S1 Nuclease Mapping of Viral RNAs from a Temperature-Sensitive Transformation Mutant of Murine Sarcoma Virus

MICHEAL NASH,[1] NICOLE V. BROWN,[1] JADE L. WONG,[1] RALPH B. ARLINGHAUS,[2] AND EDWIN C. MURPHY, JR.,[1]*

Department of Tumor Biology, Section of Virology, The University of Texas System Cancer Center, M. D. Anderson Hospital and Tumor Institute, Houston, Texas 77030,[1] and Department of Molecular Biology, Scripps Clinic and Research Foundation, La Jolla, California 92037[2]

The structures of murine sarcoma virus (MuSV) *ts*110 viral RNA and intracellular RNA present in MuSV *ts*110-infected cells (6m2 cells) have been examined by S1 nuclease analysis. A previous study involving heteroduplex analysis of MuSV *ts*110 viral RNAs hybridized to wild-type DNA revealed the presence of two MuSV *ts*110 RNAs, 4.0 and 3.5 kilobases (kb) in length, containing overlapping central deletions relative to wild-type MuSV 124 viral RNA (Junghans et al., J. Mol. Biol. **161**:229–255, 1982). Here we show that the deletion (termed Δ1) in the 4.0-kb RNA has a 5' border located at about nucleotide 2409 (using the numbering system of Van Beveren et al., Cell **27**:97–108, 1981), a position 63 bases upstream of the junction of the p30 and p10 coding sequences. The 3' border of the Δ1 deletion is found 1,473 bases downstream at approximately nucleotide 3883, 10 nucleotides downstream of the first *mos* gene initiation codon. In the 3.5-kb MuSV *ts*110 RNA, the 5' border of the deleted central region (termed Δ2) is located in a splice consensus donor site at approximately nucleotide 2017, 330 bases downstream from the junction of the p12 and p30 coding sequences, and extends about 1,915 bases in the downstream direction to nucleotide 3935, found in a splice consensus acceptor site about 55 nucleotides downstream of the first *mos* gene initiation codon and 30 bases upstream of the second initiation codon. No alteration of polyadenylate addition sites was observed in either MuSV *ts*110 RNA species, as compared with MuSV 349 RNA. The observation that the 5' and 3' borders of the deletion in the 3.5-kb RNA are within in-frame splice donor and acceptor sites suggests strongly that the 3.5-kb RNA is derived from the 4.0-kb RNA by a temperature-sensitive splice mechanism. Data presented here show unequivocally that formation of the 3.5-kb MuSV *ts*110 RNA from which the P85$^{gag-mos}$ polypeptide is translated is temperature sensitive. At 33°C, with S1 analysis, the 3.5-kb RNA is found readily in 6m2 cells. Within 4 h of a shift to 39°C, however, only trace amounts of this RNA can be found. Moreover, reshifting 6m2 cells to 33°C permits the reappearance of the 3.5-kb RNA at its original level.

Murine sarcoma virus (MuSV) *ts*110 was derived by UV irradiation of wild-type MuSV 349 virions. After infection of normal rat kidney (NRK) cells with irradiated MuSV 349 virions, an infected nonproducer cell line (6m2 cells) was derived which exhibited a transformed phenotype at 33°C and a normal phenotype at 39°C (2). At 33°C, 6m2 cells contain two virus-related proteins, P58^{gag} and P85$^{gag-mos}$, as well as two viral RNAs, ca. 4.0 and 3.5 kilobases (kb) in length (6, 16). When shifted to 39°C, 6m2 cells exhibit a normal phenotype which correlates with the disappearance of P85$^{gag-mos}$ and a significant reduction in the amount of 3.5-kb RNA (E. C. Murphy, Jr., and R. B. Arlinghaus, unpublished results). Heteroduplex mapping studies comparing the two MuSV *ts*110 RNAs to wild-type DNA showed that both contained overlapping central deletions relative to the 5.3-kb wild-type RNA. The deletion in the 4.0-kb RNA, termed Δ1, spanned about 1,560 nucleotides, extending from a 5' point about 80 nucleotides upstream of the junction of the p30 and p10 coding sequences to a 3' point at or just downstream of the beginning of the *mos* gene reading frame. The deletion in the 3.5-kb RNA, termed Δ2, spanning about 2,050 nucleotides, extended from a 5' point about 475 nucleotides upstream of the 5' border of Δ1 to a 3' point indistinguishable

from the 3' end of Δ1 (7). In vitro translation studies with MuSV *ts*110 virion RNA suggest that the P58^{gag} is translated from the 4.0-kb RNA and that P85$^{gag-mos}$ arises from the 3.5-kb RNA (7, 10). From these results we have proposed that Δ1 has fused the *gag* and *mos* genes out of frame in the 4.0-kb RNA, whereas Δ2 results in an in-frame fusion allowing the production of a *gag-mos* polypeptide, and we have noted that our data were consistent with the generation of the 3.5-kb RNA by a temperature-sensitive splicing of the 4.0-kb RNA.

In this study we show, at the level of S1 nuclease mapping, that the deletion in the 4.0-kb RNA, Δ1, results in the fusion of the p30 coding sequence to *mos* gene sequences at a point about 10 nucleotides downstream of the first *mos* initiation codon. This fusion, eliminating the first *mos* initiator, and precluding the possibility that any full-length P37^{mos} polypeptide could be made in 6m2 cells, is probably out of frame, since only P58^{gag} can be made from the 4.0-kb RNA. The deletion (Δ2) in the 3.5-kb RNA, however, extends from a splice donor site in the p30 coding sequence to an in-frame splice acceptor site in the *mos* gene about 50 bases downstream of the first *mos* initiation codon. Thus, the 3.5-kb RNA appears to contain *gag* gene and *mos* gene sequences fused in-frame and to arise, very probably, as a temperature-sensitive splice product of the 4.0-kb RNA. Additionally, kinetic data presented here establish that formation of the 3.5-kb RNA is unequivocally temperature sensitive.

---

* Corresponding author.

MATERIALS AND METHODS

Cells and viruses. Moloney (Mo)-MuSV *ts*110 was derived from Mo-MuSV 349, a subclone of Mo-MuSV 124 (1), as described by Blair et al. (2). Nonproducer NRK cells infected with Mo-MuSV *ts*110 (2), termed 6m2 cells, were maintained in McCoy 5a medium containing 15% (vol/vol) fetal calf serum or 15% newborn calf serum. MuSV *ts*110 producer cells, designated 206-2IC cells, were generated by superinfection of 6m2 cells with the IC strain of Mo-MuLV (6). These cells were maintained in the above culture medium and were used for virus production in 2-quart (1.89-liter) roller bottles.

Virus purification and viral RNA extraction. The MuSV *ts*110-MuLV virus complex was purified by high-speed centrifugation and isopycnic centrifugation (17). Mutant virus was harvested every 12 h from cultures maintained at 33°C. Viral RNA was extracted by a sodium dodecyl sulfate (SDS)-phenol-chloroform method (9) and fractionated by centrifugation in 5 to 25% sucrose gradients containing 10 mM sodium acetate (pH 5), 100 mM lithium acetate, 1 mM EDTA, and 0.1% SDS at 17,000 rpm for 18 h at 4°C in an SW27 rotor. Viral RNA (50 to 70S) was pooled, chromatographed on oligodeoxythymidylate-cellulose, ethanol precipitated, and used as a source of MuSV *ts*110 viral RNA.

DNA reagents for blot hybridization and S1 analysis. Several viral DNA subclones or fragments were used in mapping the structure of the MuSV *ts*110 viral RNA. These are diagrammed in Fig. 1 and were derived as follows.

(i) pXB.35. To construct this reagent, a 356-base pair (bp) fragment of pMLV-1 DNA (generously provided by Inder Verma) extending from an *Xho*I site at position 1560 to a *Bgl*II site at position 1906 in the Shinnick et al. (14) sequence was used. These boundaries correspond, with only eight single base mismatches, to positions 1982 to 2328 in the established MuSV 124 sequence (19). This fragment was ligated into *Xho*I-*Bgl*II-digested pKC7 DNA (13) and selected by colony hybridization after transformation of *Escherichia coli* RRI.

(ii) pNVB 1.7. A 1,717-bp fragment of MuSV 124 DNA (our original clone of full-length MuSV 124 DNA, designated p101/101, was generously given to us by Dino Dina) covering the region bounded by an *Xho*I site at position 1981 and a *Bgl*II site at position 3698 in the MuSV 124 sequence established by Van Beveren et al. (19) was subcloned into *Xho*I-*Bgl*II-digested pKC7 DNA as described above.

(iii) pBA.36. A 358-bp fragment of DNA extending from the *Bgl*II site at position 3698 to an *Ava*I site at position 4056 in the MuSV 124 sequence (19) was subcloned into *Bgl*II-*Ava*I-digested pKC7 plasmid DNA and selected as described above.

(iv) BH1.3. BH1.3 is a 1,325-bp MuSV 124 DNA fragment (see Fig. 1) extending from the *Bgl*II site at position 3698 to a *Hind*III site at position 5023.

(v) BK.68. BK.68 is a 683-bp MuSV 124 DNA fragment (see Fig. 1) extending from the *Bgl*II site at position 3698 to a *Kpn*I site at position 4381.

(vi) DD.29. DD.29 is a 290-bp fragment of pMLV-1 DNA (see Fig. 1) extending from a *Dde*I site at position 1481 to another *Dde*I site at position 1771 (14). These addresses correspond to nucleotides 1902 to 2192 in the MuSV 124 sequence (19).

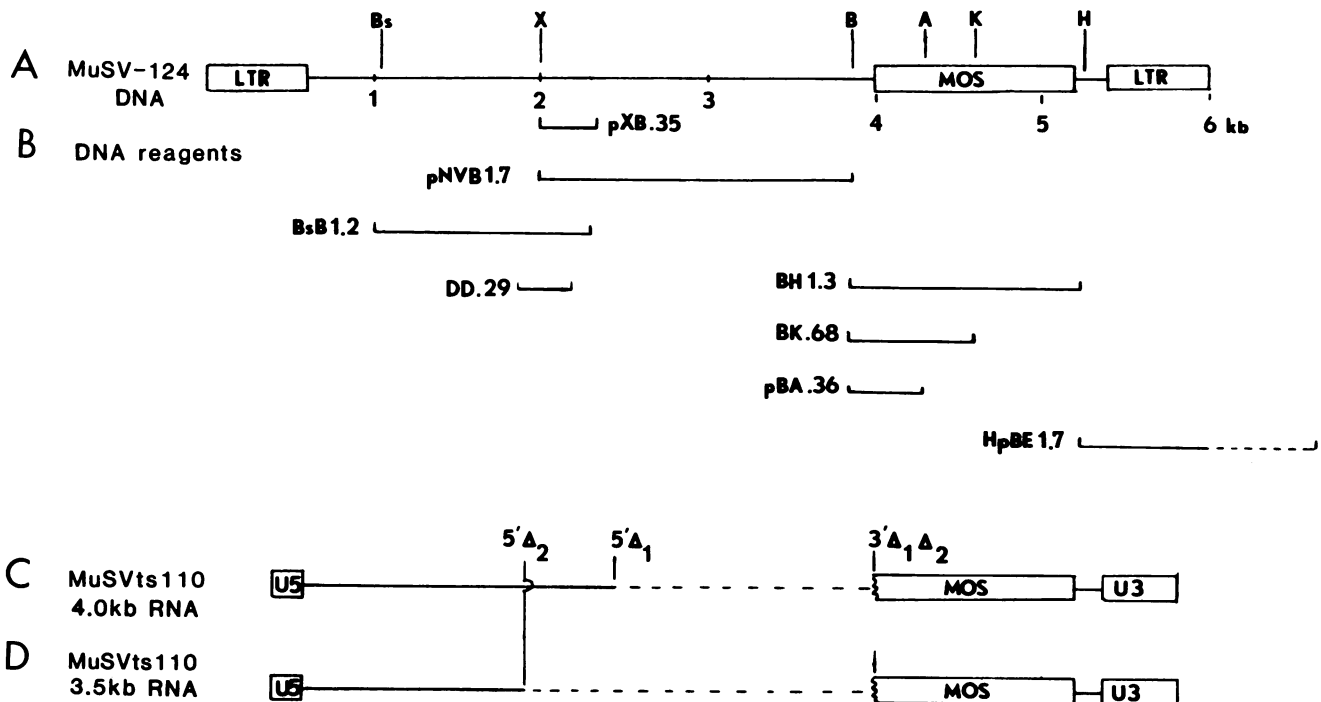**(vii) BsB1.2.** BsB1.2 is a 1,180-bp pMLV-1 DNA fragment

FIG. 1. Viral DNA and RNA structures. (A) Structure of MuSV 124 DNA (19) is shown together with the position of restriction enzyme sites relevant to this study. Bs, *Bst*EII; X, *Xho*I; B, *Bgl*II; A, *Ava*I; K, *Kpn*I; H, *Hind*III; E, *Eco*RI. (B) Viral DNA subclones and fragments used in this study for the S1 nuclease mapping of MuSV *ts*110 DNA. (C) Structure of the MuSV *ts*110 4.0-kb RNA as estimated by heteroduplex analysis (7). The limits of the central deletion (termed Δ1) relative to wild-type RNA are delineated by the symbols 5'Δ₁ and 3' Δ₁. (D) Structure of the MuSV *ts*110 3.5-kb RNA as estimated by heteroduplex analysis (7). The limits of the deletion (termed Δ2) relative to wild-type RNA are delineated by the symbols 5'Δ₂ and 3'Δ₂.

(see Fig. 1) extending from a *Bst*EII site at position 726 to a *Bgl*II site at position 1906 (14). This fragment corresponds to positions 1147 to 2328 in the MuSV 124 sequence (19).

(viii) HpBE1.7. HpBE1.7 is a 1.7-kb fragment (see Fig. 1) of MuSV 124 DNA obtained from a cDNA copy of MuSV DNA cloned by A-T tailing in the *Pst*I site of pBR322 and generously given to us by Dino Dina. This fragment contains sequences extending from the *Hin*dIII site at position 5023 through the terminus of the right-hand (3') long terminal repeat in the MuSV 124 sequence (19) and continues on to the *Eco*RI site of pBR322.

Purification of plasmid DNA. The various inserts and fragments described in the previous section were excised by digestion with the appropriate restriction enzyme(s), size fractionated on a 0.8% agarose gel, and stained with ethidium bromide. DNA was purified from agarose by adsorption to glass powder (20).

In cases where small DNA fragments were purified from polyacrylamide gels, gel slices were crushed to a paste in 2 ml of TNE buffer (10 mM Tris [pH 7.5], 100 mM NaCl, 1 mM EDTA) and agitated overnight. Acrylamide granules were removed by centrifugation, and the supernatants were filtered through Isolab QS-P columns to remove the remaining acrylamide. The column effluent containing the DNA was phenol extracted, ethanol precipitated, and dissolved in water.

Isolation of cellular RNA. Intracellular RNA was isolated from tissue culture cells by a guanidine hydrochloride extraction procedure (22). Briefly, cellular pellets were dissolved in Solution A, 8 M guanidine hydrochloride–100 mM sodium acetate (pH 5), and subjected to vigorous Dounce homogenization. After centrifugation of the extracts at 10,000 rpm for 15 min, nucleic acids were precipitated from the supernatant by addition of 0.5 volume of ethanol at −20°C for 30 min and were collected by centrifugation at 7,000 rpm for 20 min. The nucleic acid pellets were dissolved in 0.25 to 0.50 of the original volume of Solution B (Solution A + 0.1 volume of 200 mM EDTA) and again precipitated with 0.5 volume of ethanol. This last step was repeated twice more, decreasing the volume of Solution B by half each time. The final pellet was dissolved in 20 mM EDTA (pH 7.5) and extracted with chloroform-isobutanol (4:1). The aqueous phase was mixed with 2 volumes of 4.5 M sodium acetate (pH 6), and the RNA was precipitated at −20°C overnight. The RNA was collected by centrifugation, washed once with 3 M sodium acetate and once with 70% ethanol, and dissolved in water.

Preparation of cellular DNA. Cells growing in roller culture were rinsed with an isotonic buffer and gently lysed in 2% SDS–8 M urea–0.35 M NaCl–1 mM EDTA buffered with 10 mM Tris (pH 8). The cell lysate was extracted with an equal volume of phenol-chloroform (1:1) saturated with the above SDS-urea buffer and ethanol precipitated. Nucleic acids from each roller culture were dissolved in 3 to 5 ml of water, digested sequentially with 50 μg of RNase per ml at 37°C for 60 min and 100 μg of proteinase K per ml at 37°C for 120 min, re-extracted with phenol-chloroform, precipitated with ethanol, and dissolved in water.

Blot hybridization of DNA. Routinely, 15 μg of cellular DNA, digested with a given restriction enzyme as recommended by the supplier, was analyzed on a 0.8% agarose gel in 50 mM Tris (pH 8.3)–40 mM sodium acetate–2 mM EDTA at 40 V for 16 to 18 h, and was transferred to nitrocellulose essentially as described by Southern (15) and modified by Wahl et al. (21). The nitrocellulose was prehybridized at 37 to 42°C in 50% formamide–5× SSC (1× SSC is 0.15 M NaCl plus 0.015 M sodium citrate)–5× Denhardt solution (0.1% bovine serum albumin, 0.1% Ficoll, 0.1% polyvinylpyrrolidone)–0.1% SDS containing 100 μg of sheared salmon sperm DNA per ml and 2 mg of base-hydrolyzed yeast RNA per ml. Hybridization was carried out at 37 to 42°C in the same solution containing 1× Denhardt solution and 2 × 10^6 cpm of ^32P-labeled probe per ml (1 × 10^8 to 3 × 10^8 cpm/μg). After hybridization, the filters were washed four times with 3× SSC–0.1% SDS and twice with 0.1× SSC–0.1% SDS at 37°C, dried, and autoradiographed.

Blot hybridization of RNA. Cellular or viral RNA was treated with 1 M glyoxal–50% dimethyl sulfoxide–10 mM phosphate (pH 7) at 50°C for 1 h and subjected to electrophoresis (4 V/cm) on 1.2% agarose–10 mM phosphate buffer (pH 7.0). RNA in the finished gels was transferred to nitrocellulose as described by Thomas (18). Prehybridization was carried out at 37°C for 4 to 16 h in the same solution as used in the DNA blots. Hybridization was carried out at 37°C for 18 h in the same buffer containing 10% dextran sulfate and 2 × 10^6 cpm of ^32P-labeled probe per ml. After hybridization, the filters were washed four times in 2× SSC–0.1% SDS and twice in 0.1× SSC–0.1% SDS at 50°C for 15 min, dried, and autoradiographed.

End labeling of DNA. (i) 3' End labeling. The 3' ends of restricted DNA fragments were labeled by "filling in" using the Klenow fragment of DNA polymerase. Briefly, DNA fragments to be labeled (1 to 2 μg) were adjusted to 20 mM HEPES (N-2-hydroxyethylpiperazine-N'-2-ethanesulfonic acid)–7.5 mM MgCl₂–10 mM 2-mercaptoethanol–50 μg of bovine serum albumin per ml. To this mixture was added 2.5 μl (6 to 8 U) of the Klenow fragment of DNA polymerase, 40 μCi of the appropriate α-^32P-deoxynucleoside triphosphate (>3,000 Ci/mmol), and 0.1 mM unlabeled deoxynucleoside triphosphates as required by the restriction site to be filled in. After incubation at 15°C for 60 min, 20 mM EDTA was added to stop the reaction. The reaction mix was desalted by passage over a G-50 column equilibrated in TNE buffer after the addition of 20 μg of carrier DNA. Radioactivity in the void volume was pooled, ethanol precipitated, and dissolved in TE buffer (10 mM Tris [pH 8], 1 mM EDTA).

(ii) 5' End labeling. Restriction fragments were first dephosphorylated with calf intestinal phosphatase (Boehringer Mannheim Biochemicals). Briefly, DNA was adjusted to 50 mM Tris (pH 9)–1 mM MgCl₂–0.1 mM ZnCl₂–1 mM spermidine containing 10 U of calf intestinal phosphatase at 37°C. After 30 min, an additional 10 U of calf intestinal phosphatase was added for another 30 min. The digest was mixed with 0.1 volume of 10× TNE buffer and 0.05 volume of 10% SDS for 15 min at 68°C to halt the reaction. After phenol-chloroform (1:1) extraction, the nucleic acids were ethanol precipitated. For 5' end labeling, dephosphorylated DNA was adjusted to 100 mM Tris (pH 7.6)–120 mM MgCl₂–10 mM dithiothreitol–0.2 mM spermidine–0.2 mM EDTA, to which was added 10 to 20 U of T4 kinase and 150 μCi of [γ-^32P]ATP for 1 h at 37°C. The reaction mix was desalted on a G-50 column, and the end-labeled DNA was collected as described for 3' end labeling.

Hybridization and S1 nuclease digestion. End-labeled DNA and RNA (usually 0.1 μg of viral RNA or 10 μg of intracellular RNA) were mixed and ethanol precipitated together with sufficient purified yeast RNA to bring the nucleic acid amount up to 100 μg. The pellets were thoroughly dissolved in 30 μl of 80% formamide–40 mM PIPES [piperazine-N,N'-bis(ethanesulfonic acid)] (pH 6.8)–400 mM NaCl–1 mM EDTA, immersed in an 85°C water bath for 15 min, and transferred to a water bath at the hybridization temperature

(52 to 56°C, depending on the G-C content of the DNA probe) for 3 h. After hybridization, 300 μl of 50 mM sodium acetate (pH 4.6)–280 mM NaCl–4.5 mM ZnSO₄–20 μg of single-stranded DNA per ml containing 200 U of S1 nuclease (P-L Biochemicals) per ml was added for 30 min at 37°C. S1 digestion was stopped by the addition of 50 μl of 4 M ammonium acetate–0.1 mM EDTA, and the digests were extracted once with phenol-chloroform (1:1). The aqueous phase was ethanol precipitated after the addition of 20 μg of carrier yeast RNA.

Analysis of S1 digests. For size analysis of protected DNA fragments, S1 digests were dissolved in 10 to 25 μl of urea loading buffer (10 M urea, 1 mM EDTA, 0.1 N NaOH, 0.015% bromocresol green), heated to 50°C for 5 min, applied to a 10- to 30-cm 4% polyacrylamide gel (prepared by using a 30% acrylamide–1.6% bisacrylamide stock) containing 8 M urea, and subjected to electrophoresis at 80 to 125 V for 16 to 18 h. End-labeled DNA markers (pBR322 DNA cut with either *Alu*I or *Hinf*I) were run in parallel lanes as standards. Finished gels were briefly fixed with 50% methanol–7% acetic acid, dried, and autoradiographed. From the degree of separation of the standard DNA fragments, we estimated the degree of error in our measurements to be ±5 bases.

RESULTS

Positions of the 3' borders of Δ1 and Δ2. In previous work (7), heteroduplexes formed between MuSV 124 DNA and MuSV *ts*110 viral RNAs suggested that the 3' borders of both Δ1 and Δ2 mapped at or just downstream from the beginning of the *mos* gene open reading frame (see Fig. 1C and D for the approximate positioning of the deletion borders). In vitro translation experiments supported these data since fragmented MuSV *ts*110 viral RNA is primarily translated into P33^{mos} rather than into full-length P37^{mos} by using the second *mos* gene initiation codon positioned 96 bases downstream of the first initiation codon (10). It should be noted that full-length MuSV *ts*110 RNA is translated to form P58^{gag} and P85$^{gag-mos}$. Fragmented MuSV *ts*110 RNA, however, as well as fragmented wild-type MuSV 124 RNA (10, 11), can use the internal initiation sites in the *mos* gene for the translation of *mos* gene polypeptide products.

To map more precisely the 3' deletion boundaries, we first employed a 5'-end-labeled 1,325-bp fragment of MuSV 124 DNA (the BH1.3 fragment in Fig. 1B) extending from a *Bgl*II site 176 bp upstream of the *mos* gene to a *Hind*III site 28 bp downstream. In Fig. 2A, the sizes of DNA fragments protected from S1 digestion in hybrids formed between fragment BH1.3 and MuSV 349 viral RNA, MuSV *ts*110 viral RNA, 6m2 cellular RNA, and 206-2IC cellular RNA are shown. As expected, MuSV 349 viral RNA protected the entire BH1.3 fragment (Fig. 2A, lane 2). Hybridization to MuSV *ts*110 RNA (Fig. 2A, lane 3) and 206-2IC intracellular RNA (Fig. 2A, lane 5), in contrast, yielded two size classes of protected fragments, estimated to be ca. 1,140 and 1,100 bases long. A small amount of fully protected BH1.3 DNA was also observed. Intracellular RNA from 6m2 cells protected only the 1,140- and 1,100-base fragments (Fig. 2A, lane 4); no full-size BH1.3 DNA was protected. The 1,140- and 1,100-base fragments of BH1.3 DNA protected by MuSV *ts*110 RNA correspond to deletion points just downstream of the first *mos* initiation codon, which is itself 1,148 nucleotides upstream of the 5'-end-labeled *Hind*III site. Both deletions, however, map upstream of the second *mos* gene initiation codon at position 3968, which is 1,055 nucleotides upstream of the *Hind*III site. We interpret the protection of a

small amount of full-size BH1.3 DNA by MuSV *ts*110 viral RNA and 206-2IC cellular RNA (Fig. 2A, lanes 3 and 5) as an artifact for the following reasons. The BH1.3 fragment contains 176 bases of helper sequences extending from the *Bgl*II site downstream to just beyond the first *mos* initiation codon. These sequences would be expected to hybridize to helper MuLV RNA. However, the hybrid would never be detected unless MuSV RNA were available to hybridize to the labeled *mos* gene end of the probe. For these reasons, we propose that the small amount of full protection observed in these experiments is due to an S1 nuclease-resistant mixed hybrid containing MuLV RNA, MuSV *ts*110 RNA, and the probe. As would be predicted by this reasoning, RNA from a helper-minus cell line such as 6m2 would not protect full-size BH1.3, as is the case (Fig. 2A, lane 4).

We were initially surprised to find that MuSV *ts*110 RNA appeared to contain two RNA species with different deletion points within the *mos* gene, since our heteroduplex study had predicted essentially indistinguishable 3' deletion points, although in our heteroduplex results (7) there was a hint that there might be two 3' deletion borders 10 bases apart. To test the results shown above and to provide more precise measurements of the deletion points, we employed two other *mos* DNA fragments in S1 nuclease protection experiments. In Fig. 2B are shown the results of an experiment in which MuSV 349, MuSV *ts*110, and 6m2 cellular RNA were hybridized to a 5'-end-labeled 683-bp *Kpn*I to *Bgl*II *mos* DNA fragment (fragment BK.68 in Fig. 1B), and the S1 nuclease-resistant DNA was displayed on an acrylamide gel. MuSV 349 RNA, as expected, protected the entire BK.68 fragment (data not shown). MuSV *ts*110 (Fig. 2B, lane 2) and 6m2 cellular RNA (Fig. 2B, lane 3) each protected two DNA fragments estimated to be 495 and 450 bases in length. These results are consistent with those observed using the BH1.3 fragment (Fig. 2A) and place one deletion point 12 bases downstream of the first *mos* initiator and the other 45 bases further downstream. In a third experiment (Fig. 2C), a 5'-labeled 358-bp *Ava*I-*Bgl*II fragment (pBA.36 in Fig. 1B) was also hybridized to MuSV *ts*110 and 6m2 cellular RNA. Again, two DNA fragments were protected by MuSV *ts*110 RNA; the lengths of the protected DNA fragments were estimated to be 175 and 122 bases (Fig. 2C, lane 1).

From the results presented above, we were able to obtain a consensus for the 3' deletion points in both the MuSV *ts*110 RNA species (Fig. 3). The sequences shown in Fig. 3 are excerpted from the wild-type MuSV 124 sequence (19) and are presented with the assumption that the MuSV *ts*110 genome differs from the wild-type genome only in the Δ1 and Δ2 deletions discussed here. With this assumption as a premise, it is apparent that one MuSV *ts*110 RNA species has a 3' deletion point estimated to be 8 to 11 bases downstream of the first *mos* initiation codon. The other MuSV *ts*110 RNA species has a 3' deletion border positioned between 48 and 62 bases downstream of the first *mos* initiator. Interestingly, this last deletion maps within a *mos* gene sequence (underlined in Fig. 3) which is an excellent match for a consensus splice acceptor sequence, $(_T^C)_n N_T^C AG/G$ (8).

It was crucial to establish which of the known 4.0- and 3.5-kb MuSV *ts*110 RNA species contained which *mos* gene deletion. Accordingly, two experiments were done to establish these relationships. In the first experiment, 6m2 cells growing at 33°C were shifted to 39°C for various periods of time. In this experiment, based on previous results (6), we would expect to observe a drastic diminution of the 3.5-kb RNA from which P85$^{gag-mos}$ is translated. In the second

FIG. 2. Analysis of the 3' deletion borders in MuSV ts110 RNA. RNA was obtained from wild-type MuSV 349 virions, MuSV ts110 virions, 6m2 cells, or 206-2IC cells were hybridized to either 5'-end-labeled DNA fragment BH1.3, BK.68, or pBA.36 (see Fig. 1). The hybrids were digested with S1 nuclease, and the protected fragments were analyzed on a 4% polyacrylamide gel containing 8 M urea. (A) 5'-End-labeled BH1.3 DNA protected from S1 digestion by hybridization to (lane 2) MuSV 349 viral RNA, (lane 3) MuSV ts110 viral RNA, (lane 4) 6m2 intracellular RNA, and (lane 5) 206-2IC intracellular RNA. Lane 1 represents a size standard of a 5'-end-labeled HinfI-digest of pBR322 DNA. (B) 5'-End-labeled BK.68 DNA protected from S1 digestion by hybridization to (lane 2) MuSV ts110 viral RNA, and (lane 3) 6m2 intracellular RNA. Lane 1 is the pBR322-HinfI standard. (C) 5'-end-labeled pBA.36 DNA protected from S1 digestion by hybridization to (lane 1) MuSV ts110 viral RNA and (lane 2) MuSV 349 viral RNA. Positions of the size standards are shown alongside lane 1.

FIG. 3. Locations of the two 3' deletion borders in MuSV ts110 RNA in relation to the nucleotide sequence of wild-type MuSV 124 DNA. By using sequence data obtained by Van Beveren et al. (19), the positions of the two 3' deletions (Δ) in MuSV ts110 RNA are designated in relation to the first and second mos gene initiation codons and to a consensus splice acceptor sequence found between positions 3920 and 3940 in the MuSV 124 sequence. The three arrows used for each deletion point represent the actual deletion point observed with DNA fragment BH1.3, BK.68, or pBA.36.

experiment, 6m2 cells growing at 33°C were shifted to 39°C and then back to 33°C. In this experiment, we expected to observe the disappearance at 39°C and then reappearance at 33°C of the 3.3-kb RNA. These temperature-dependent fluctuations in the 3.5-kb RNA should be reflected in a similar fluctuation of one of the protected DNA fragments. RNA was prepared from the shifted 6m2 cells and hybridized to 5′-end-labeled pBA.36 insert. RNA from 6m2 cells growing at 33°C protected both the 175- and 122-base fragments from S1 nuclease digestion (Fig. 4A, lane 2), as does MuSV *ts*110 viral RNA (Fig. 4A, lane 7). Progressive lengths of shift to 39°C, however, resulted in the gradual failure to protect the smaller, 122-base DNA fragment from S1 nuclease digestion (Fig. 4A, lanes 3 through 6), arguing that the 3.5-kb MuSV *ts*110 RNA contained the larger *mos* gene deletion whose 3′ border mapped in a splice acceptor sequence (see Fig. 3). In these experiments, there is a fairly substantial amount of probe which appears to be fully protected (note the fragment migrating at about 350 bases in Fig. 4A and 4B). This is an experimental artifact resulting from the fact that hybridization was done in DNA excess to provide an accurate estimate of the amount of hybridizing MuSV *ts*110 RNA species. Control experiments to which DNA alone was added showed a similar amount of fully protected DNA (data not shown). In the second experiment, in addition to its predicted disappearance after a 24-h shift to 39°C (Fig. 4B, lane 2), the 122-base DNA fragment and, hence, the RNA with the larger *mos* deletion reappeared in 6m2 cells shifted back to 33°C for 24 h from 39°C (Fig. 4B, lane 3). In previous work (6) we have established that P85*gag-mos* disappears and the 3.5-kb RNA is drastically reduced in 6m2 cells shifted to 39°C (E. C. Murphy, Jr., and R. B. Arlinghaus, unpublished results) and, significantly, both reappear upon a reshift to 33°C. Hence, we are confident that the 3.5-kb MuSV *ts*110 RNA contains the larger *mos* gene deletion.

Position of the 5′ borders of Δ1 and Δ2. From our heterodu-

plex maps (7), the 4.0-kb MuSV *ts*110 RNA contains ca. 1,560-base deletion extending from a point about two-thirds of the way through the p30 coding sequence to a point just inside the *mos* gene. From the S1 nuclease protection results shown in Fig. 2 and 4 and summarized in Fig. 3, the 3′ border of Δ1 (4.0-kb RNA) corresponds to about nucleotide 3885 in the MuSV 124 sequence. Calculating back from this point, the 1,560-base deletion should have a 5′ border near nucleotide 2325 in the MuSV 124 sequence, and Δ2 (3.5-kb RNA), originally estimated by us to be about 2,050 bases long (7), should extend in the 5′ direction from nucleotide 3935 to a 5′ border near nucleotide 1885 in the MuSV 124 sequence.

Our early experiments confirmed that the 5′ borders of Δ1 and Δ2 lay in approximately the positions predicted by the heteroduplex experiments. We subcloned a fragment of the MuLV *gag* gene corresponding to nucleotides 1981 to 2328 in the MuSV 124 *gag* gene sequence (plasmid pXB.35 in Fig. 1). Based on the predicted 5′ deletion borders, nucleotide 1885 in Δ2 and 2325 in Δ1 (see Fig. 1C and 1D), the insert in this subclone should hybridize selectively to the RNA containing Δ1. i.e., the 4.0-kb MuSV *ts*110 RNA. A blot hybridization experiment (Fig. 5) confirmed this prediction. Only the 4.0-kb MuSV *ts*110 RNA (Fig. 5, lane 1) would hybridize to the pXB.35 insert, although both RNAs hybridized to a *mos* gene probe (Fig. 5, lane 2). From these data we could predict that the 5′ border of Δ1 lay somewhere within the sequence homologous to the 357-base insert in pXB.35 and that the 5′ border of Δ2 lay somewhere upstream of nucleotide 1981.

Using this information, we prepared two DNA reagents designed to map the 5′ borders of Δ1 and Δ2. The first of these was a subclone of MuSV 124 DNA, designated pNVB 1.7 (see Fig. 1B). The insert in this plasmid extended from the *Xho*I site at position 1981 to the *Bgl*II site at position 3698, and thus should span only the 5′ border of Δ1. No hybrid should be observed with the Δ2-containing 3.5-kb RNA. S1 digests of the hybrid formed between the 3′- end-
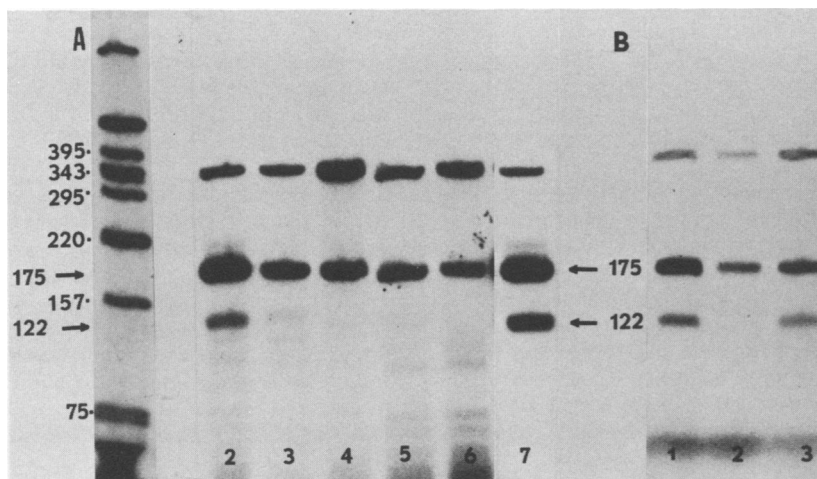

FIG. 4. Correlation of the two 3′ deletion borders with the 4.0- and 3.5-kb MuSV *ts*110 RNAs. 6m2 cells growing at 33°C were shifted to 39°C for periods of time from 4 h through 48 h, and RNA was prepared from the cells. Alternately, 6m2 cells growing at 33°C were shifted to 39°C for 24 h and then shifted back to 33°C. RNA was prepared from the cells at all three points. The various RNAs were hybridized to 5′-end-labeled pBA.36 DNA. The hybrids were digested with S1 nuclease, and the protected fragments were displayed on a 4% polyacrylamide gel containing 8 M urea. (A) 5′-End-labeled pBA.36 DNA protected from S1 digestion by hybridization to RNA obtained from (lane 2) 6m2 cells at 33°C, (lane 3) 6m2 cells shifted to 39°C for 4 h, (lane 4) 6m2 cells shifted to 39°C for 8 h, (lane 5) 6m2 cells shifted to 39°C for 24 h, (lane 6) 6m2 cells shifted to 39°C for 48 h, and (lane 7) MuSV *ts*110 viral RNA. Lane 1 is the pBR322-*Hinf*I standard. (B) 5′-End-labeled pBA.36 DNA protected from S1 digestion by hybridization to RNA obtained from (lane 1) 6m2 cells at 33°C, (lane 2) 6m2 cells shifted to 39°C for 24 h, and (lane 3) 6m2 cells shifted to 39°C for 24 h and then back to 33°C for 24 h.
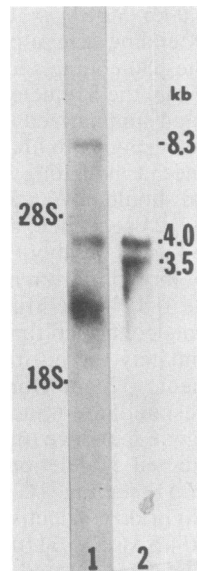
FIG. 5. Viral DNA which hybridizes specifically to the 4.0-kb MuSV *ts*110 RNA. MuSV *ts*110 viral RNA was size fractionated on a 1.2% agarose gel after denaturation with 1 M glyoxal–50% dimethyl sulfoxide, transferred to nitrocellulose, and hybridized either to (lane 1) the pXB.35 insert or to (lane 2) a *mos* gene probe equivalent to fragment BH1.3 in Fig. 1.

labeled pNVB 1.7 insert, MuSV *ts*110 viral RNA, 6m2. cellular RNA, and 206-IC cellular RNA revealed the protection of a 430-bp fragment (Fig. 6A, lanes 3, 4, and 5). Predictably, MuSV 349 viral RNA protected the entire 1.7-kb pNVB 1.7 insert (Fig. 6A, lane 2). Additionally, S1-resistant hybrids formed between the probe and MuLV helper sequences were observed near 1,700 and 800 bases when using MuSV *ts*110 viral RNA and 206-2IC cellular RNA (Fig. 6A, lanes 3 and 5) but not in helper-minus 6m2 cellular RNA (Fig. 6A, lane 4). From these data we conclude that the 5' border of Δ1 is found at a position corresponding to approximately nucleotide 2409 in the MuSV 124 sequence, 430 bases downstream from the reference *Xho*I site at position 1981. Thus, by S1 mapping, we find the 4.0-kb MuSV *ts*110 RNA to contain a 1,476-base central deletion relative to wild-type 5,323-base MuSV 124 RNA, the deletion extending from nucleotide 2409 in the p30 coding sequence to nucleotide 3885 in the v-*mos* gene, yielding a 3,850-base viral RNA, minus the polyadenylate sequence. Since this RNA is translated to form P58^{gag}, we assume that the *gag-mos* fusion yields an out-of-frame *mos* sequence.

Because of the relative positions of the 5' borders of Δ1 and Δ2, it was not possible to generate a DNA reagent which would hybridize selectively to the Δ2 RNA. To map the Δ2 5' border, we prepared several *Dde*I fragments of pMLV-1 which spanned the region around nucleotide 1885, the predicted Δ2 5' border. Our first experiment, utilizing a 550-bp pMLV-1 *Dde*I fragment within which nucleotide 1885 lay, was unsuccessful in the sense that it was fully protected from S1 digestion by hybridization to MuSV *ts*110 RNA (data not shown). Hybridization of the next downstream fragment, however, a 290-bp fragment (designated DD.29), spanning nucleotides 1902 to 2192 of the MuSV 124 sequence, to MuSV *ts*110 RNA showed some full protection of the 290-base probe and a substantial amount of protection of a 120-base fragment (Fig. 6B, lane 1). As expected, hybridization

of DD.29 to MuSV 349 RNA protected the entire fragment from S1 digestion (Fig. 6B, lane 2). These results place the 5' border of Δ2 at about nucleotide 2022, 120 bases downstream of the reference *Dde*I site at nucleotide 1902. Significantly, there is an excellent consensus splice donor site— CAG/GTAGG (the consensus sequence is $^C_AAG/GT^A_GGT[8]$)— spanning nucleotides 2015 to 2022 in the wild-type MuSV 124. Splicing of this donor site to the acceptor site found at the 3' end of the Δ2 deletion (see Fig. 3) would result in a continuous *gag-mos* open reading frame (see Fig. 9).

Polyadenylate addition sites in MuSV *ts*110 RNA. Considering the foregoing data, it seems quite possible that the 3.5-kb MuSV *ts*110 RNA is a splice product of the 4.0-kb RNA, using splice donor and acceptor sites that are present but unutilized in wild-type viral RNA. Because alternate splice patterns can be a consequence of or related to changes in polyadenylation sites (4), we mapped the 3' termini in the wild-type and MuSV *ts*110 viral transcripts. For this experiment we hybridized both wild-type and MuSV *ts*110 viral RNA, as well as 6m2 cellular RNA, to a 3'-end-labeled DNA fragment (HpBE 1.7 in Fig. 1B), starting at a *Hind*III site at nucleotide 5022 just downstream of the *mos* gene, extending across the 3' long terminal repeat and continuing into vector pBR322 sequences. As shown in Fig. 7 lanes 2, 3, and 4, a 740-base fragment of the HpBE 1.7 DNA was protected from S1 digestion by all the RNAs employed, placing the 3' termini of both the wild-type and MuSV *ts*110 RNA at a position about 23 bases downstream of an AATAAA polyadenylation signal (5, 12) found at nucleotides 5735 to 5740 in the MSV 124 DNA sequence (19). Since there is another AATAAA polyadenylation signal at nucleotides 5208 to 5213 in the MuSV 124 sequence, about 190 bases downstream from the *Hind*III site, it is probable that the protection of a 175-base fragment of the probe in Fig. 7, lanes 2, 3, and 4, is a result of a small proportion of the MuSV 349 and MuSV *ts*110 RNA species being polyadenylated near this site. From these data, it appears that, whatever polyadenylation signals are used, they are identical in MuSV 349 and MuSV *ts*110. Hence, the novel splice pattern proposed in MuSV *ts*110 is not a consequence of an alteration in the 3' terminus of the viral RNA.

Proviral DNA in MuSV *ts*110-infected cells. The splice mechanism proposed above is predicted on the assumption that only one MuSV *ts*110 viral DNA is integrated into the genome of the NRK host cells. To test this assumption, high-molecular-weight cellular DNA from uninfected NRK-2 cells and MuSV *ts*110-infected 6m2 cells was digested with *Bam*HI, size fractionated on an agarose gel, transferred to nitrocellulose, and hybridized to a v-*mos* probe. Uninfected NRK-2 cellular DNA contains a single ca. 23-kb *mos*-related DNA fragment (Fig. 8, lane 1). This fragment is presumed to represent the c-*mos* gene. MuSV *ts*110-infected 6m2 cells, on the other hand, contain a 12.8-kb *mos*-related DNA fragment (Fig. 8, lane 2) in addition to the 23-kb c-*mos* fragment. This 12.8-kb *mos*-related fragment also hybridized to a MuLV and long terminal repeat probe (data not shown). Because of the greater intensity of the 12.8-kb v-*mos* fragment relative to the single-copy c-*mos* fragment, it seemed possible that the 12.8-kb DNA might contain multiple hybridizing species. To test this possibility, 6m2 DNA was double digested with *Bam*HI and *Sst*I. Based on the sequence of MuSV 124, *Sst*I was expected to cut once in each viral long terminal repeat (19). When digested in this way, 6m2 DNA yielded a *mos*$^+$ DNA species about 4.0 kb in size, exactly the size predicted to yield the 4.0-kb MuSV *ts*110. However, molecular cloning of DNA from revertant MuSV
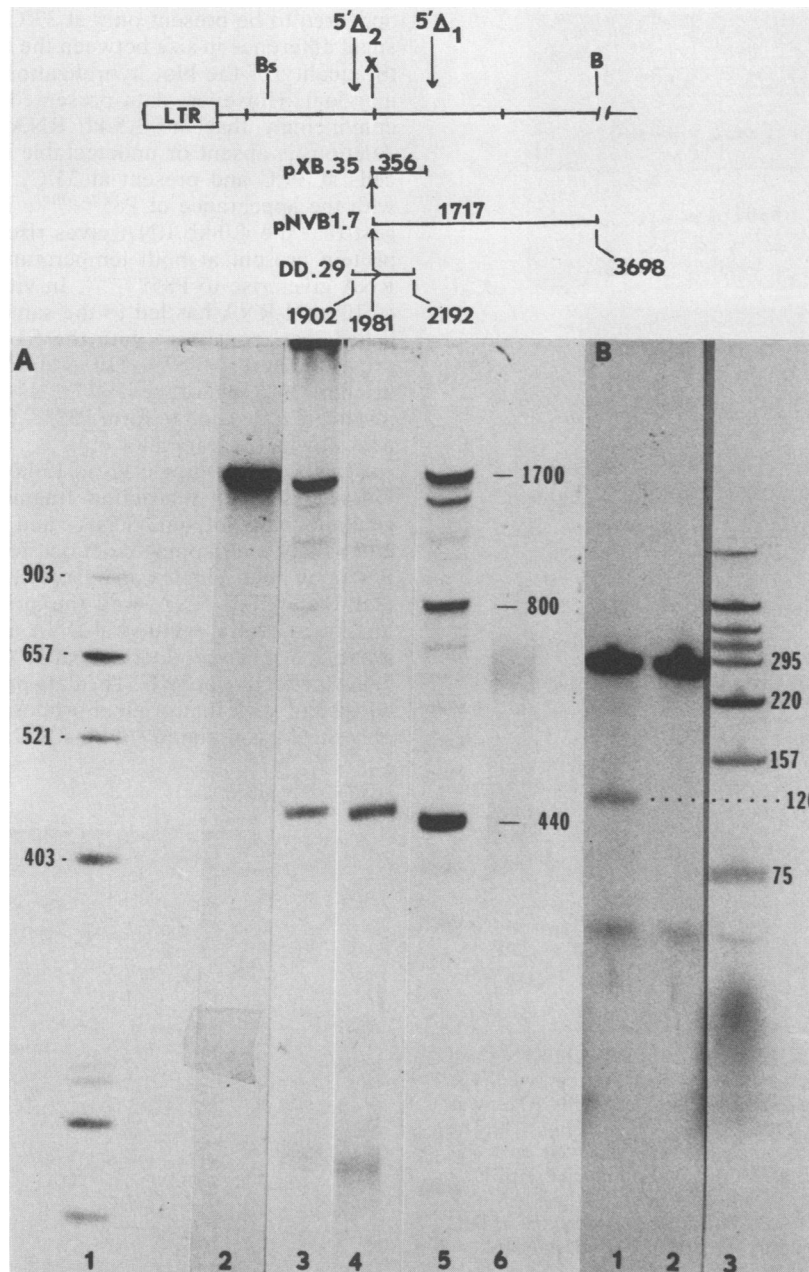
FIG. 6. Analysis of the 5' deletion borders in MuSV *ts*110 RNA. RNA from wild-type MuSV 349 virions, MuSV *ts*110 virions, 6m2 cells, or 206-2IC cells was hybridized to either 3'-end-labeled pNVB 1.7 DNA or DD.29 DNA (see Fig. 1). The hybrids were digested with S1 nuclease and displayed on a 4% polyacrylamide gel containing 8 M urea. (A) 3'-End-labeled pNVB 1.7 DNA protected from S1 digestion by hybridization to (lane 2) MuSV 349 viral RNA, (lane 3) MuSV *ts*110 viral RNA, (lane 4) 6m2 intracellular RNA, and (lane 5) 206-2IC intracellular RNA. Lane 1 contains a 5'-End-labeled *Alu*I digest of pBR322 DNA. (B) 3'-End-labeled DD.29 DNA protected from S1 digestion by hybridization to (lane 1) MuSV *ts*110 viral RNA and (lane 2) MuSV 349 viral RNA. Lane 3 contains the pBR322-*Hin*fI digest.

*ts*110 cell lines has revealed the presence of a 5.2-kb *mos*⁺ *Sst*I fragment within the 12- to 13-kb *Bam*HI v-*mos* DNA fragment. The 5.2-kb DNA exhibits a restriction map identical to the wild-type MuSV 124 DNA, and molecular clones containing this DNA can transform NIH 3T3 cells (B. Brizzard, D. Blair and E. C. Murphy, Jr., unpublished results). We can, however, find no evidence for either transcription of a 5.2-kb viral RNA or synthesis of wild-type Pr63*ᵍᵃᵍ* in any MuSV *ts*110-infected cell line. From these results we tentatively conclude that the 12.8-kb region of

*Bam*HI-digested revertant DNA contains two viral DNAs on separate fragments. One fragment contains a ca. 4.0-kb viral genome (as an *Sst*I fragment) which can be transcribed into the MuSV *ts*110 4.0-kb RNA which, in turn, can be spliced at 33°C to form the 3.5-kb RNA. The other contains a 5.2-kb wild-type-like viral genome which is inactive.

DISCUSSION

Our original interest in MuSV *ts*110 stemmed from the fact that cells infected with this viral mutant display a trans-
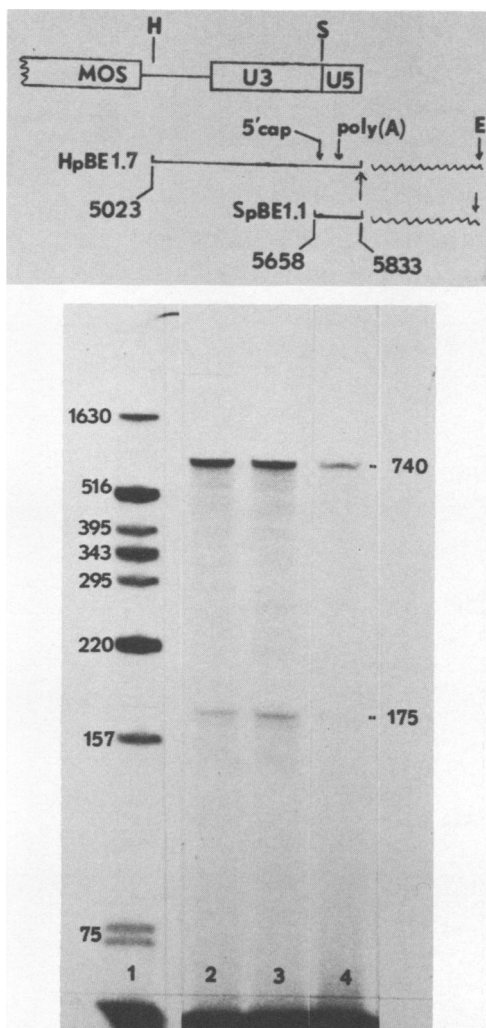
FIG. 7. Determination of the 3' termini in MuSV *ts*110 RNA and wild-type MuSV 349 viral RNA. RNA obtained from wild-type MuSV 349 virions, MuSV *ts*110 virions, and 6m2 cells RNA was hybridized to 3'-end-labeled HpBE1.7 DNA (see Fig. 1). The hybrids were digested with S1 nuclease and displayed on a 4% polyacrylamide gel containing 8 M urea. 3'-End-labeled HpBE1.7 DNA protected from S1 digestion by hybridization to (lane 2) MuSV 349 viral RNA, (lane 3) MuSV *ts*110 viral RNA, and (lane 4) 6m2 intracellular RNA. Lane 1 contains the pBR322-*Hin*fI standard.

formed phenotype at 33°C but revert to normal morphology at 39°C, offering the possibility that a comparative analysis of viral nucleic acids and proteins at the permissive and nonpermissive temperatures would be instructive with regard to how the v-*mos* gene functions in transformed cells.

We have shown in previous studies that, in experiments in which cells are shifted from 39°C to 33°C and vice versa, the appearance of the transformed phenotype correlates positively with the synthesis and accumulation of a *gag* gene-*mos* gene fusion protein, designated P85$^{gag-mos}$ (23). Actinomycin D can block the appearance of P85$^{gag-mos}$, which argues that de novo synthesis of a viral RNA is necessary for its synthesis (3, 6). In addition, blot hybridization analysis of 6m2 intracellular RNA at the permissive and nonpermissive temperatures has shown the presence of a 4.0-kb viral RNA at both 33 and 39°C, together with a 3.5-kb viral RNA which

appeared to be present only at 33°C (6, 16). Because of the small difference in size between the two MuSV *ts*110 RNAs, the quality of the blot hybridization experiments has been marginal. However, data presented in this study establish convincingly that the 3.5-kb RNA, containing the larger deletion, is absent or undetectable in MuSV *ts*110-infected cells at 39°C and present at 33°C, thus correlating strictly with the appearance of P85$^{gag-mos}$. These observations suggest that the 4.0-kb RNA gives rise only to P58^{gag}, a viral protein present at both temperatures, and that the 3.5-kb RNA gives rise to P85$^{gag-mos}$. In vitro translation of MuSV *ts*110 viral RNA has led to the same conclusion and established that, consistent with the S1 nuclease mapping data presented here, MuSV *ts*110 viral RNA cannot be translated in vitro into wild-type P37^{mos} as well as P85$^{gag-mos}$ but instead is translated to form P33^{mos} (and P85$^{gag-mos}$) from the next downstream initiator (10).

Because only a single 12- to 13-kb transcriptionally active v-*mos*-containing restriction fragment has been found in genomic blots of 6m2 DNA, and because of the nearly completely overlapping deletions found in the MuSV *ts*110 RNAs by heteroduplex analysis (7), it was considered likely that the 4.0-kb RNA was the primary transcript of the integrated MuSV *ts*110 viral DNA and that the 3.5-kb RNA arose as a splice product only at 33°C, the splicing somehow being ineffective at 39°C. The data presented in this study are consistent with that original proposal, showing that at 39°C only the Δ1-containing 4.0-kb RNA is found in MuSV *ts*110-
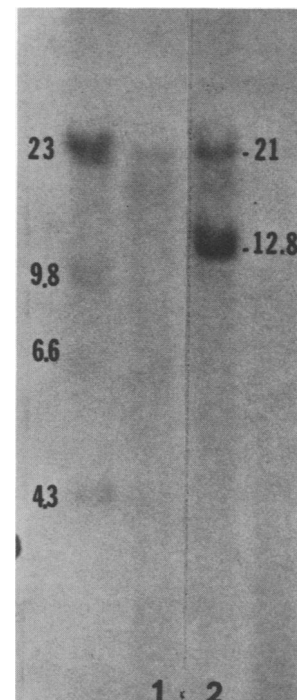

FIG. 8. Blot hybridization of NRK and 6m2 genomic DNA to a *mos* gene probe. High-molecular-weight genomic DNA obtained from uninfected NRK-2 cells and MuSV *ts*110-infected 6m2 cells were digested with *Bam*HI, analyzed on an 0.8% agarose gel, transferred to nitrocellulose, and hybridized to a ^{32}P-labeled *mos* probe. (Lane 1) Hybrids formed between the NRK-2 DNA *Bam*HI digest and the *mos* probe; (lane 2) hybrids formed between the 6m2 DNA *Bam*HI digest and the *mos* probe. The unmarked lane represents a trace amount of end-labeled λDNA digested with *Hin*dIII.

infected cells. A shift to 33°C, however, results in the appearance of the Δ2 3.5-kb RNA. Conversely, a shift to 39°C from 33°C results in the virtually complete disappearance of the 3.5-kb RNA. As thus far elucidated, the structure of the two MuSV *ts*110 RNA species is consistent with the proposed temperature-sensitive splicing mechanism.

Based on the available data, a summary of what is known about the MuSV *ts*110 RNAs is shown in Fig. 9. Although the positions of the proposed deletion points are located exactly in our model, it must be emphasized that our S1 nuclease analysis is accurate only to within ±5 nucleotides. Additionally, the model presented in Fig. 9 is based on the assumption that, with the exception of a central deletion, the nucleotide sequence of MuSV *ts*110 is identical to the published MuSV 124 sequence (19). In recent experiments performed to refine our data, primer extension nucleotide sequence analysis (M. Nash, unpublished results) has suggested that, in the MuSV *ts*110 4.0-kb RNA, the 5' (*gag*) end of the deletion occurs out of frame at nucleotide 2404 (our S1 analysis placed it in the vicinity of nucleotide 2409) and the 3' (*mos*) end of the deletion occurs at nucleotide 3892 (S1

analysis placed it near nucleotide 3883). Upstream and downstream of the *gag* gene-*mos* gene junction, the sequence of MuSV *ts*110 appears to be identical to MuSV 124. In the MuSV *ts*110 3.5-kb RNA, the 3' end of the deletion appears to be exactly at the proposed intron-exon border at nucleotide 3936 in the *mos* gene. Experiments are under way to extend the sequence across the *gag-mos* junction in the 3.5-kb RNA.

Subject to these limitations, a model for the MuSV *ts*110 system is presented in Fig. 9. Wild-type MuSV 124 RNA is ca. 5,320 bases long (19). Relative to this wild-type RNA (shown in Fig. 9 as a full-length DNA so that the nucleotide addresses given below would mesh with the published sequence), the MuSV *ts*110 4.0-kb RNA, as estimated by S1 analysis, contains a central deletion (Δ1) of about 1,470 bases. This result is in good agreement with our original estimate of 1,560 ± 110 bases for Δ1 by heteroduplexing (7). Thus, minus the polyadenylate tract, the MuSV *ts*110 4.0-kb RNA is estimated to be about 3,850 bases long. Because the MuSV *ts*110 4.0-kb RNA can only be translated into P58^{gag} and P33^{mos} in vitro (10), this deletion has resulted in a out-of-
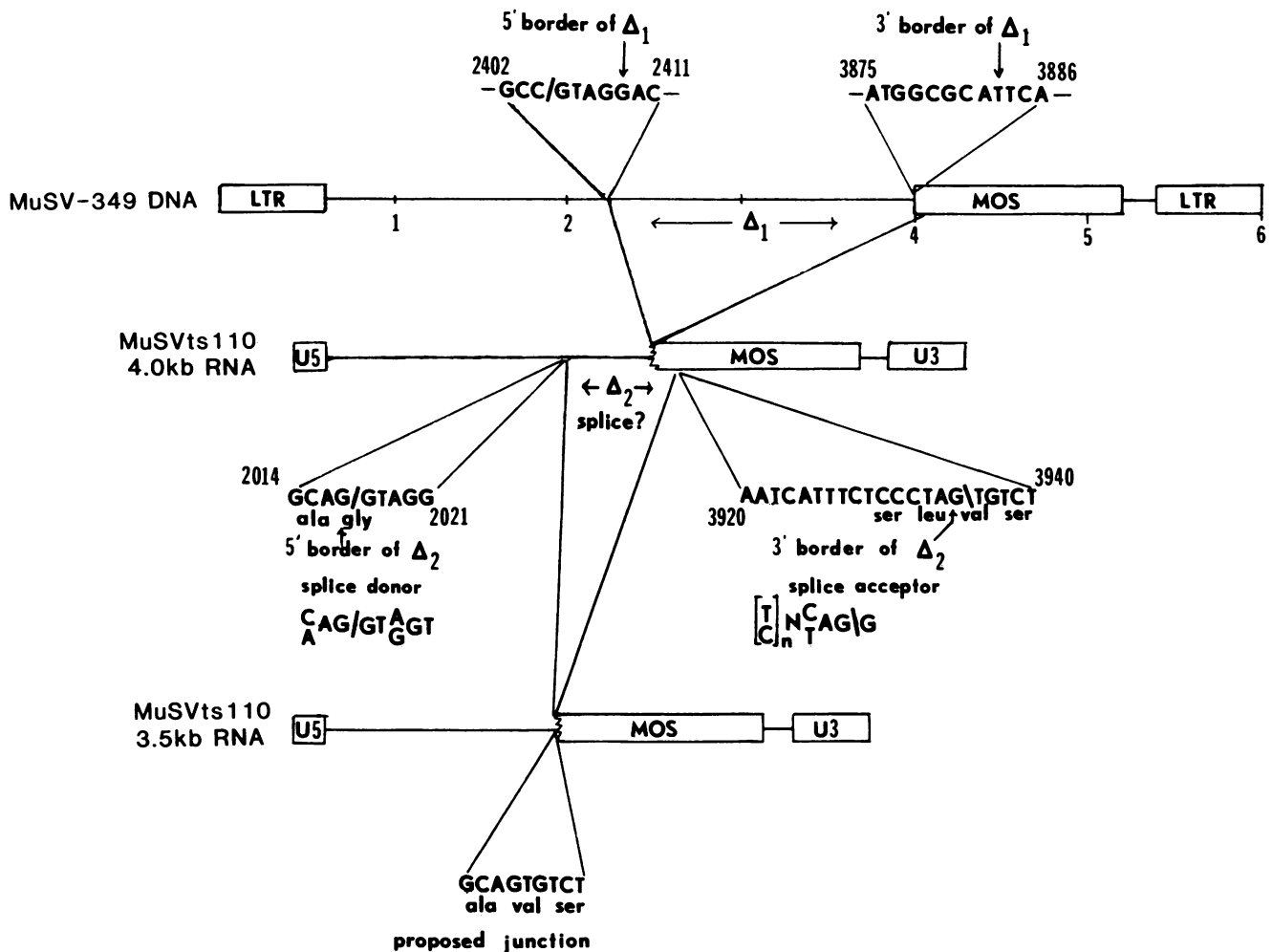

FIG. 9. Proposed locations of the 5' and 3' deletion borders in the MuSV *ts*110 4.0- and 3.5-kb RNAs in relation to the nucleotide sequence of wild-type MuSV 124 DNA. Using the Van Beveren et al. (19) sequence data, the MuSV *ts*110 4.0-kb RNA is shown to contain ca. 1,476-base deletion (designated Δ1) corresponding to an excision of the nucleotide sequence between positions 2409 and 3883 in the MuSV 124 sequence. The MuSV *ts*110 3.5-kb RNA contains a deletion estimated at 1,922 bases (designated Δ2), bounded by a consensus splice donor sequence at position 2013 to 2021 and a consensus splice acceptor sequence at position 3925 to 3936.

frame fusion of the *gag* and *mos* genes, eliminating the first *mos* gene initiation codon. There is a recognizable but somewhat poorly matched splice donor site (GCC/GTAG) at nucleotides 2402 to 2408 in the MuSV 124 sequence (19), placing an exon-intron border only about five nucleotides upstream of the 5' border of Δ1 as mapped in this study. Inspection of the MuSV 124 sequence around the 3' border of Δ1, however, fails to reveal any nearby candidate splice acceptor site, with the possible exception of the sequence CCATCCTCTAG/A between positions 3858 and 3869 (19). This acceptor sequence, however, is upstream of the first *mos* initiation codon (nucleotide 3875), and its use would contradict both the S1 data presented here and previously published in vitro translation data (10), which argue against the presence of the first *mos* initiation codon in MuSV *ts*110 RNA. Thus, our evidence weighs against the MuSV *ts*110 4.0-kb RNA being a splice product of a still larger primary transcript.

By using the same calculations that were applied to the MuSV *ts*110 4.0-kb RNA, the MuSV *ts*110 3.5-kb RNA contains ca. 1,990-base deletion, resulting in an RNA about 3,235 bases long in which *gag* and *mos* sequences are also fused. In contrast to the 4.0-kb RNA, however, the points of fusion appear to be at recognizable in-frame splice donor and acceptor sites. For example, as shown in Fig. 9, at the 3' (*mos*) end of the deletion in the 3.5-kb RNA, there is an excellent consensus splice acceptor match between nucleotides 3920 and 3940 in the MuSV 124 sequence. At the 5' end of this same deletion, there is a well-matched splice donor sequence (see Fig. 9). Removal of the intron and joining of the donor and acceptor sites would result in the formation of a 3.4- to 3.5-kb RNA with a continuous *gag* gene-*mos* gene open reading frame (see Fig. 9).

Further studies in this system are sure to be interesting. Clones of integrated viral DNA are now being developed from 6m2 cells and from revertant cell lines in which the splice mechanism appears to be insensitive to temperature shifts. Comparative studies of the nucleotide sequence at the *gag* gene-*mos* gene junctions should yield interesting information regarding the nature of the splicing mechanisms in general.

ACKNOWLEDGMENTS

LITERATURE CITED

1. **Ball, J. K., J. A. McCarter, and S. M. Sunderland.** 1982. Evidence for helper-independent murine sarcoma virus. I. Segregation of replication-defective viruses. Virology **56**:268–284.
2. **Blair, D. G., M. A. Hull, and E. A. Finch.** 1979. The isolation and preliminary characterization of temperature-sensitive transformation mutants of Moloney sarcoma virus. Virology **95**:303–316.
3. **Brown, R., J. P. Horn, L. Wible, R. B. Arlinghaus, and B. R. Brinkley.** 1981. Analyses of the sequence of events in the transformation process in cells infected with a ts transformation mutant of Moloney murine sarcoma virus. Proc. Natl. Acad. Sci. U.S.A. **78**:5593–5597.
4. **Darnell, J. E., Jr.** 1982. Variety in the level of gene control in eukaryotic cells. Nature (London) **297**:365–371.
5. **Fitzgerald, M., and T. Shenk.** 1981. The sequence 5'-AAUAAA-3' forms part of the recognition site for polyadenylation of late SV40 mRNAs. Cell **24**:251–260.
6. **Horn, J. P., T. G. Wood, E. C. Murphy, Jr., D. G. Blair, and R. B. Arlinghaus.** 1981. A selective temperature-sensitive defect in viral RNA. Expression in cells infected with a ts transformation mutant of murine sarcoma virus. Cell **25**:37–46.
7. **Junghans, R. P., E. C. Murphy, Jr., and R. B. Arlinghaus.** 1982. Electron microscopic analysis of ts110 Moloney mouse sarcoma virus, a variant of wild-type virus with two RNAs containing large deletions. J. Mol. Biol. **161**:229–255.
8. **Mount, S. M.** 1982. A catalogue of splice junction sequences. Nucleic Acids Res. **10**:459–472.
9. **Murphy, E. C., Jr., and R. B. Arlinghaus.** 1978. Cell-free synthesis of Rauscher murine leukemia virus "gag" and "gag-pol" precursor polyproteins from virion 35S RNA in a mRNA-dependent translation system derived from mouse tissue culture cells. Virology **86**:326–343.
10. **Murphy, E. C., Jr., and R. B. Arlinghaus.** 1982. Comparative tryptic peptide analysis of candidate P85$^{gag-mos}$ of ts110 Moloney murine sarcoma virus and P38-P23 *mos* gene-related proteins of wild-type virus. Virology **121**:372–383.
11. **Papkoff, J., M. H. T. Lai, T. Hunter, and I. Verma.** 1981. Analysis of transforming gene products from Moloney murine sarcoma virus. Cell **27**:109–119.
12. **Proudfoot, N. J., and G. G. Brownlee.** 1976. 3' Non-coding region sequences in eukaryotic messenger RNA. Nature (London) **263**:211–214.
13. **Rao, R. N., and S. G. Rogers.** 1979. Plasmid pKC7: a vector containing ten restriction endonuclease sites suitable for cloning DNA segments. Gene **7**:79–82.
14. **Shinnick, T. M., R. A. Lerner, and J. G. Sutcliffe.** 1981. Nucleotide sequence of Moloney murine leukaemia virus. Nature (London) **293**:543–548.
15. **Southern, E. M.** 1975. Detection of specific sequences among DNA fragments separated by gel electrophoresis. J. Mol. Biol. **98**:503–517.
16. **Stanker, L. H., J. P. Horn, G. E. Gallick, W. S. Kloetzer, E. C. Murphy, Jr., D. G. Blair, and R. B. Arlinghaus.** 1983. gag-mos polyproteins encoded by variants of the Moloney strain of mouse sarcoma virus. Virology **126**:336–347.
17. **Syrewicz, J. J., R. B. Naso, C. S. Wang, and R. B. Arlinghaus.** 1972. Purification of large amounts of murine ribonucleic acid tumor viruses produced in roller bottle cultures. Appl. Microbiol. **24**:488–498.
18. **Thomas, P. S.** 1980. Hybridization of denatured RNA and small DNA fragments transferred to nitrocellulose. Proc. Natl. Acad. Sci. U.S.A. **77**:5201–5205.
19. **Van Beveren, C., F. van Straaten, J. A. Galleshaw, and I. M. Verma.** 1981. Nucleotide sequence of the genome of a murine sarcoma virus. Cell **27**:97–108.
20. **Vogelstein, B., and D. Gillespie.** 1979. Preparative and analytical purification of DNA from agarose. Proc. Natl. Acad. Sci. U.S.A. **76**:615–619.
21. **Wahl, G. M., M. Stern, and G. R. Stark.** 1979. Efficient transfer of large DNA fragments from agarose gels to diazobenzyloxymethyl-paper and rapid hybridization by using dextran sulfate. Proc. Natl. Acad. Sci. U.S.A. **76**:3683–3687.
22. **Westin, E. H., F. Wong-Staal, E. P. Gelmann, R. D. Favera, T. S. Papas, J. A. Lautenberger, A. Eva, E. Premkumar Reddy, S. R. Tronick, S. A. Aaronson, and R. C. Gallo.** 1982. Expression of cellular homologues of retroviral *onc* genes in human hematopoietic cells. Proc. Natl. Acad. Sci. U.S.A. **79**:2490–2494.
23. **Wood, T. G., J. P. Horn, W. G. Robey, D. G. Blair, and R. B. Arlinghaus.** 1980. Characterization of viral specified proteins present in NRK cells infected with a temperature-sensitive transformation mutant of Moloney murine sarcoma virus. Cold Spring Harbor Symp. Quant. Biol. **44**:747–754.